J Nanopart Res (2012) 14:1274
DOI 10.1007/s11051-012-1274-x

RESEARCH PAPER

Convenient preparation of ITO nanoparticles inks for transparent conductive thin films

Daisuke Ito · Keiichiro Masuko · Benjamin A. Weintraub · Lallie C. McKenzie · James E. Hutchison

Received: 14 January 2012 / Accepted: 30 October 2012 / Published online: 15 November 2012

Abstract Tin-doped indium oxide (ITO) nanoparticles are useful precursors to transparent electrodes in a variety of technologically important applications. We synthesized ITO nanoparticles from indium and tin acetylacetonates in oleyl alcohol using a novel temperature ramp profile. The monodispersed ITO nanoparticles have an average diameter of 8.6 nm and form dense, flat films by simple spin coating. The thickness of the film can be controlled by varying the number of additional depositions. The resulting ITO film is transparent and has a resistivity of 7×10^{-3} Ω cm after sintering at 300 °C. Using a suitable solvent, it is possible to coat high-aspect-ratio structures with ITO nanoparticles. This approach to ITO coatings is greener and offers a number of advantages for transparent electrodes because it is highly versatile, easily scalable, and supports low-cost manufacturing.

Keywords ITO · Nanoparticles · Greener manufacturing · Transparent electrodes · Coatings

This article is part of the topical collection on nanomaterials in energy, health and environment

D. Ito · K. Masuko · B. A. Weintraub · L. C. McKenzie · J. E. Hutchison
Nanoscience Open Research Initiative, Materials Science Institute, University of Oregon, Eugene, OR 97403, USA
e-mail: hutch@uoregon.edu

D. Ito · K. Masuko · B. A. Weintraub · L. C. McKenzie · J. E. Hutchison
Department of Chemistry, University of Oregon, Eugene, OR 97403, USA

D. Ito (✉)
Nano Science Research Laboratory, US Research Center, Sony Electronics Inc., Eugene, OR 97403, USA
e-mail: daisukeb.ito@jp.sony.com

Introduction

Transparent electrodes are important materials that have been intensively investigated over the last decade (Hecht et al. 2011). Tin-doped indium oxide (ITO) (Tahar et al. 1998) is the most successful transparent electrode material for a wide variety of applications including displays (Bechinger et al. 1996), functional glasses (Bechinger et al. 1996; Chen et al. 2005), solar cells (Krebs 2009; Zhu et al. 2011), and light-emitting diodes (Chen et al. 2005; Ho et al. 2000; Ho and Granström 1998). The increased demand for ITO due to the rapid expansion of these applications makes the cost of ITO films a serious concern for industry. Thus, finding alternative transparent electrode materials or optimizing the processes for producing ITO films are emerging priorities in materials science and engineering (Minami 2005; Argun et al. 2003; Tvingstedt and Inganäs 2007; Otabe et al. 1998; Kim et al. 2009). Developing improved processes is the best solution in the short term because it is difficult to replace ITO because of the requirements for commercial applications that include not only "conductivity and transparency" but also "total

cost, productivity, and reliability" (Spaid 2012). For ITO films, the total cost is influenced not only by the price of indium itself but also the inefficiencies of the deposition methods (e.g., sputtering methods). In fact, only 15 % of the indium source is typically utilized in the production of transparent electrodes in devices (Hecht et al. 2011; Li et al. 2011). In addition, sputtering deposition chambers have become larger and more expensive to fabricate large devices with high productivity. Recycling of the ITO waste introduces extra cost. Thus, there is the opportunity to replace the current deposition methods for ITO with more cost-effective deposition processes.

One of the promising routes for cost-effective production is the solution deposition of ITO films. Because a precursor "ink" can be used to deposit ITO films, existing roll-to-roll or ink-jet systems can be utilized for low-cost, reduced-waste, highly scalable, and high speed manufacturing (Chen et al. 2005; Bühler et al. 2007; Jeong et al. 2010). Compared to metal organic depositions of ITO precursors that require crystallization sintering at over 500 °C where thermal damage can occur to other components of the device, films formed from ITO nanoparticles do not require high temperature sintering because crystalline nanoparticles are already formed during chemical production. In addition, nanoparticle inks capped by organic ligands can be stable with reliable quality (Ba et al. 2006; Gilstrap et al. 2008; Sun et al. 2010). Given these advantages, interest in ITO nanoparticle inks has steadily increased (Bühler et al. 2007; Jeong et al. 2010; Goebbert et al. 1999; Ba et al. 2006; Gilstrap et al. 2008). Although solution deposition of ITO nanoparticle ink is a simple pathway to fabricate ITO thin films, a key step is to produce ITO nanoparticles with high crystallinity and homogeneous composition.

There are several reports of syntheses of monodispersed ITO nanoparticles (Bühler et al. 2007; Ba et al. 2006; Gilstrap et al. 2008; Sun et al. 2010). In a typical synthesis, pyrolysis of metal organic precursors is conducted in a high boiling point organic solvent. The decomposition of the metal salt generates nuclei that subsequently grow into well-defined nanoparticles. However, tight control of the reaction conditions is required to avoid undesirable side reactions. The need for such control of the reaction conditions is a practical disadvantage of these syntheses for producing nanoparticle inks.

Recently, Caruntu et al. has reported synthesis of In_2O_3 nanoparticles using oleyl alcohol as a solvent in air (Caruntu et al. 2010), but did not report tin-doping of these nanoparticles using this approach. In general, impurity doping by pyrolysis is difficult because each metal precursor has a different decomposition temperature. In this article, we have synthesized monodispersed ITO nanoparticles from indium acetylacetonate in oleyl alcohol in air by a unique temperature profile. Since oleyl alcohol is a non-toxic alcohol, this route offers the added benefit that it reduces environmental risks. In addition, we demonstrate characteristics of ITO nanoparticle films as transparent conductive films. The ITO nanoparticle films are able to deposit uniformly onto high-aspect-ratio structures.

Experimental

Synthesis of ITO nanoparticles

All chemicals were purchased from Sigma Aldrich. Indium (III) acetylacetonate (99.9 %, 0.45 mmol) and tin(II) acetylacetonate (99.9 %, 0.05 mmol) were mixed with 12.5 mL of oleyl alcohol at room temperature in a 50 mL three-neck round-bottom flask under a flowing stream of air (Caruntu et al. 2010). The reaction mixture was heated to 200 °C and kept for 30 min to dissolve all of precursors, then heated to 260 °C at a rate of 2 °C/min and maintained at 260 °C for 30 min under flowing of nitrogen to nucleate ITO clusters. Since the mixture of indium and tin precursors easily forms aggregated precipitation, 30 min of aging at 260 °C is important to form ITO clusters. During the aging at 260 °C, the color of the reaction mixture changed slowly from a light yellow to a dark blown. The solution temperature was then increased to 320 °C and maintained for 1.5 h. During the aging at 320 °C, the color of the reaction mixture changed from a dark brown to a dark blue solution. The resulting solution was cooled to room temperature, 25 mL of ethanol and 5 mL of methanol were added to precipitate the nanoparticles and the particles were isolated by centrifugation for 30 min at 7,500 rpm. The solid product was washed six times with ethanol and then dispersed in toluene. The resulting toluene dispersion was centrifuged for five min at 3,500 rpm to remove any insoluble solids.

Synthesis of ZnO nanopillars

ZnO nanopillar substrates were fabricated on Si substrates by a gold-nanoparticles-catalyzed vapor–liquid–solid method as described previously (Ito et al.

2008). In brief, ZnO seed films were prepared by spin casting a sol–gel Zn precursor onto Si wafers with a 3-μm thermal SiO_2 layer, followed by an annealing step. A mixture of ZnO and carbon powder (roughly 1:1 by mass) was placed in a small quartz tube as a ZnO source, and the ZnO substrate was placed downstream from the source. The substrate temperature was held constant at 600 °C. The source temperature was raised to 900 °C and held for 20 min in N_2 gas flow (2.5 SCFH). Then, the furnace was shut down and cooled to room temperature while maintaining the nitrogen flow.

Deposition of ITO nanoparticles

An ITO nanoparticle ink was prepared by dissolving the ITO nanoparticles (10 % of Sn) in a mixture of toluene and 1-octanol (1:20 by volume). Films were deposited from this ink on glass substrates or ZnO nanopillar substrates using a spin coating (3,000 rpm).

Measurements

Transmission electron microscope (TEM) observation was carried out with a FEI Titan operated at 300 kV. Measurements of size distribution of nanocrystals are expressed as a function of the standard deviations. TEM and X-ray photoelectron spectra (XPS) samples were prepared by drop-casting onto a holey carbon grid and Si substrates, respectively. XPS was carried out with a Thermo Scientific ESCALAB 250 X-ray Photoelectron Spectrometer using an aluminum X-ray source. The binding energy scale of all measurements was calibrated using the C_{1s} peak at 284.8 eV. SEM was carried out using a ZEISS Ultra-55.

Results and discussion

To synthesize nearly monodispersed ITO nanoparticles in oleyl alcohol, careful control of reaction temperature is necessary. Figure 1 shows the temperature profile used to synthesize monodispersed ITO nanoparticles from the acetylacetonate complexes in oleyl alcohol. If the heating rate is higher than 3 °C/min, a precipitation of black powder (a mixture of indium metal, In_2O_3, and SnO_2) occurs. By way of contrast, in the case of In_2O_3 nanoparticles, any heating rate lower than 5 °C/min is acceptable. In that case, the temperature of the

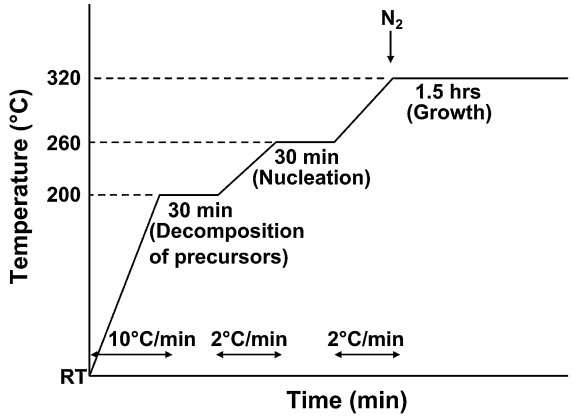

Fig. 1 The temperature profile of the reaction mixture for production of monodispersed In_2O_3 and ITO nanoparticles from acetylacetonate precursors in oleyl alcohol. The blanketing gas is changed from air to nitrogen at 320 °C

precipitation is about 260 °C which corresponds with the nucleation temperature of In_2O_3 clusters (Caruntu et al. 2010). The nucleation step of ITO clusters is critical to control the generation of dispersed ITO nanoparticles. After the initial nucleation of ITO clusters is completed during an aging at 260 °C for 30 min, no precipitation occurs. Introduction of a nitrogen atmosphere during aging at 320 °C is also an important step for ITO nanoparticles because heating in this inert environment introduces oxygen vacancies in the ITO nanoparticles that enhance electric conductivity. Aging under air makes color of ITO nanoparticle solution brown.

Figure 2a and b show TEM images of In_2O_3 and 10 % tin-doped ITO nanoparticles, respectively. The images reveal that both In_2O_3 and ITO nanoparticles are nearly monodisperse and exhibit no aggregation. Measurements of 150 random particles indicate average diameters of 7.0 nm (±0.7 nm) for In_2O_3 and 8.6 nm (±0.9 nm) for ITO, both with narrow size distributions (Fig. 6c, d). The colors of In_2O_3 and ITO nanoparticle solutions are yellow and blue, respectively (insets of Fig. 7c, d). The color of ITO solution is the result of the effects of doping by tin impurities.

Figure 3a, b show selected area electron diffraction (SAED) patterns of In_2O_3 and ITO nanoparticles, respectively. The diffraction patterns indicate that the matrix phase of both types of nanoparticles is cubic In_2O_3 without any different phases. There is no SnO_2 phase in ITO. Figure 3c, d show high-resolution TEM images of In_2O_3 and ITO nanoparticles, respectively. These images suggest that both types of nanoparticle are single crystal.

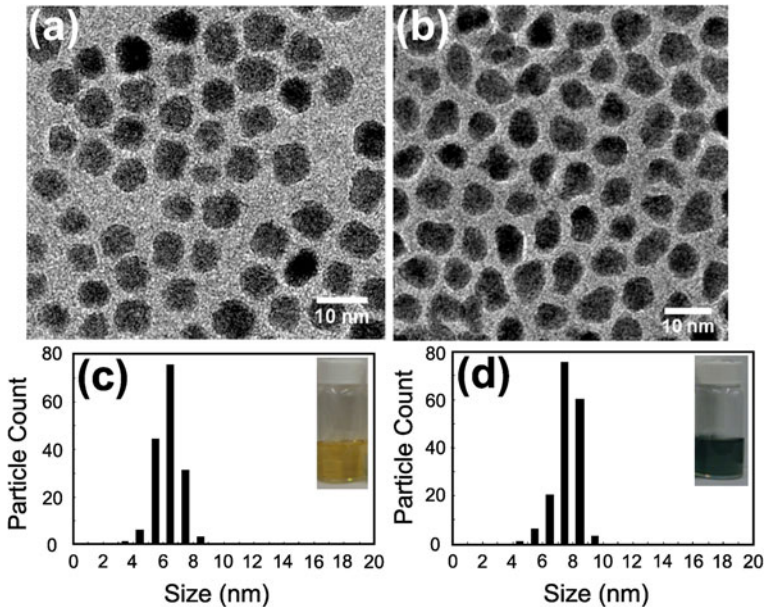

Fig. 2 TEM images of **a** In_2O_3 and **b** 10 % tin-doped ITO nanoparticles synthesized at 320 °C in oleyl alcohol. Size distribution analyses of **c** In_2O_3 and **d** ITO; Those *insets* show optical photographs of In_2O_3 and ITO nanoparticles solution

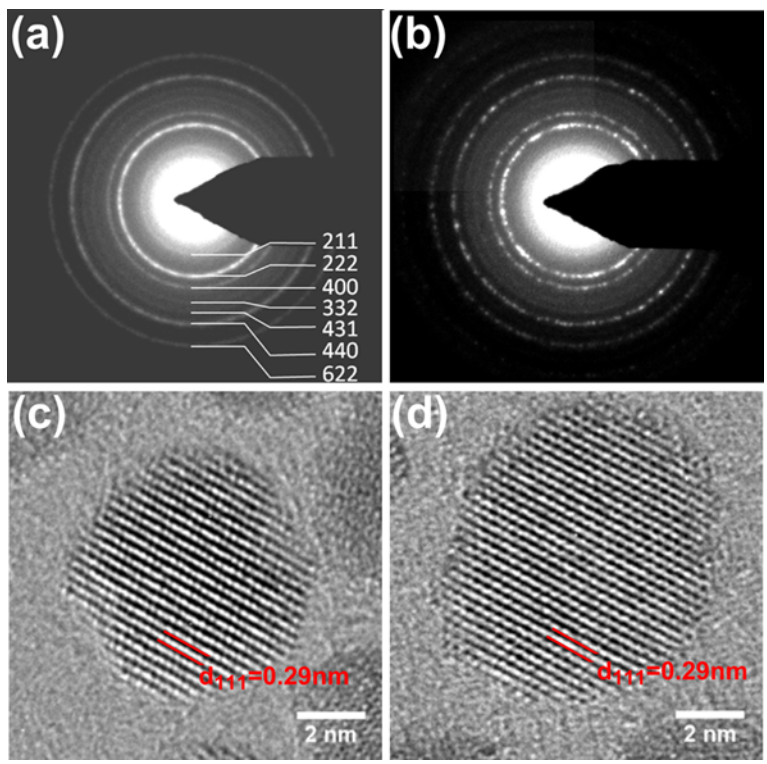

Fig. 3 Selected area electron diffraction patterns of **a** In_2O_3 and **b** ITO nanoparticles and high-resolution TEM images of **c** In_2O_3 and **d** ITO nanoparticles

Figure 4 shows normalized XPS of the O_{1s} core levels for ITO nanoparticles. The binding energy scale of all measurements was calibrated using the C_{1s} peak at 284.8 eV. Peaks of O_{1s} shift approximately 0.4 eV toward high binding energy by adding tin into In_2O_3 matrix. The peaks can be assigned based upon literature reports for ITO. Peak I of O_{1s} at 529.6 eV ± 0.2 eV is due to bulk O^{2-} ions whose neighboring indium atoms possessed a full complement of six nearest O^{2-} ions, and peak II at 530.6 ± 0.2 eV corresponds to O^{2-} ions in

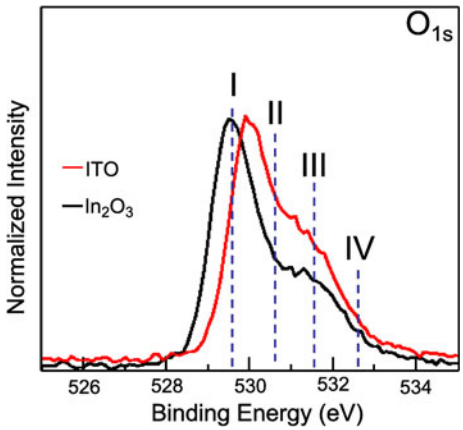

Fig. 4 XPS spectra of In_2O_3 and ITO nanoparticles. $O1_s$ spectra overlaid for comparison (The counts of the largest peak in each of the two spectra were normalized)

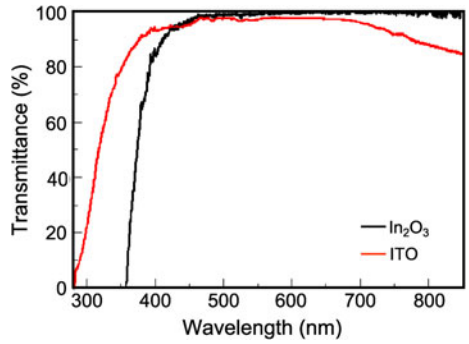

Fig. 5 UV–Vis transmission spectra of In_2O_3 and ITO nanoparticle solutions

oxygen deficiency regions (Donley et al. 2002). Peaks III and IV at 531.6 ± 0.2 eV and 532.6 ± 0.2 eV are assigned to InOOH or $In(OH)_3$ and absorbed H_2O or contaminants (Donley et al. 2002), respectively. Tin-doping into In_2O_3 matrix causes a decrease of peak I and increases in peaks II and III, which indicates introduction of oxygen vacancies and surface defects. These results are consistent with the idea that the effect of tin-doping is not only substitution of indium sites but also introduction of oxygen vacancies (Fan and Goodenough 1977; Lin et al. 2005). The oxygen vacancies also work as n-type dopants to enhance conductivity. The results of XPS suggest that the oxygen vacancies are a result of the tin-dopant ions.

Figure 5a shows UV–Vis transmission spectra of In_2O_3 and ITO nanoparticles solutions. Both solutions are transparent throughout most of the visible range. The UV–Vis spectra of the ITO nanoparticles solution show absorptions at longer wavelength that are likely the result of free-electron vibrations (Gilstrap and Summers 2009) of highly conductive materials. The blue shift of the bandgap absorption in ITO nanoparticles relative to In_2O_3 nanoparticles can be explained by Burstein-Moss effect (increasing of free-electron density). Taken together, these results suggest that the ITO nanoparticles are optically semiconducting, but electrically metallic even though the size is below 10 nm.

We have produced transparent electrodes by depositing ITO nanoparticles films from the ITO nanoparticle ink. A suitable ink was produced by dispersing the ITO nanoparticles in a mixture of toluene and 1-octanol (1:20 by volume). ITO nanoparticle films were deposited by spin coating onto Si or glass substrates and the samples were annealed at 300 °C to remove the surface ligands of the nanoparticles. The thickness of the film can be increased by performing additional depositions, each followed by annealing at 300 °C. Figure 6a, b shows an optical photograph and a cross-section SEM image of an ITO nanoparticle film, respectively. The ITO film (thickness: 110 nm) is transparent in visible range and the film consists of nearly close-packed ITO nanoparticles. Figure 6c, d show a UV–Vis transmission spectrum and the dependence of electric conductivity of the In_2O_3 and ITO nanoparticle films upon the post-deposition annealing temperature. The ITO nanoparticle film has 98 % of transparency in the visible range and has a similar spectrum to the ITO nanoparticle solution. Electrical resistivity values of In_2O_3 and 10 % tin-doped ITO nanoparticles films after annealing at 300 °C show 1×10^2 and 7×10^{-3} Ω cm, respectively. The difference of resistivity with and without tin-doping is larger than 10,000 times.

We aimed to investigate whether these inks could also be deposited on non-planar substrates. Figure 7 shows SEM images of ITO nanoparticles deposited by spin coating on a substrate containing vertical ZnO nanopillars (Ito et al. 2008). Since 1-octanol is highly wettable on oxide surfaces, the ITO nanoparticle ink in 1-octanol is able to be deposited onto ZnO nanopillars. After repeating the spin coating (five times), ZnO nanopillars are completely coated by ITO nanoparticles film from the bottoms to tips. These results show that, in comparison with conventional sputtering methods, ITO inks can be deposited onto high-aspect-ratio structures or porous structures if ITO inks can penetrate into structures.

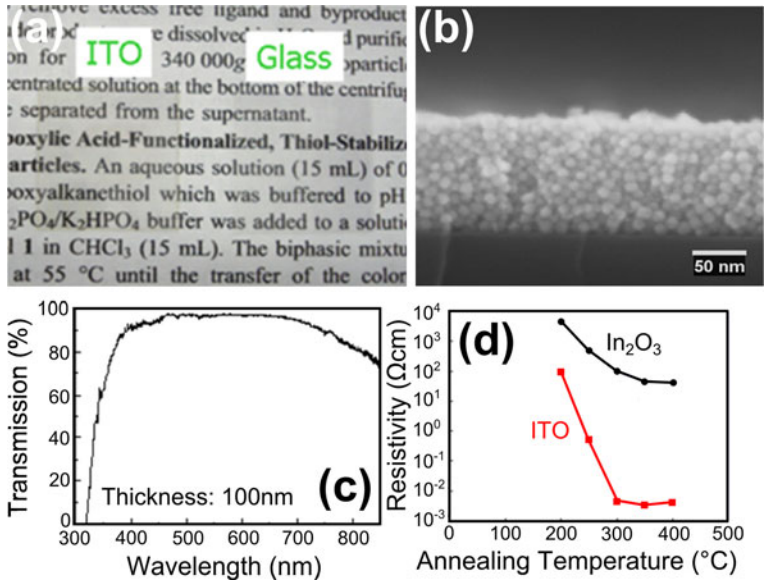

Fig. 6 **a** An optical photograph, **b** a cross-section SEM image, and **c** a UV–Vis transmission spectrum of the ITO nanoparticle film. **d** Dependence of the electric conductivity of In_2O_3 and ITO nanoparticle films on the post-deposition annealing temperature

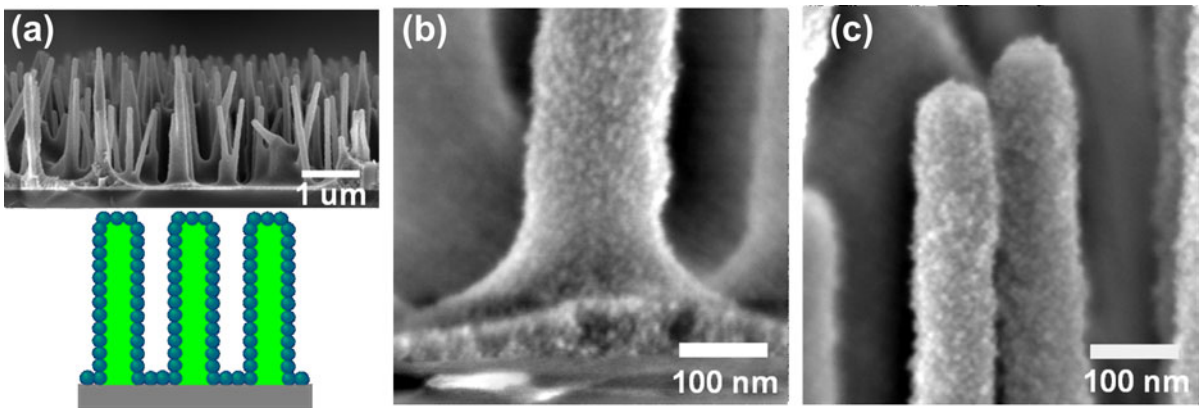

Fig. 7 Cross-section SEM images of ITO nanoparticles coating onto a ZnO nanopillar substrate. **a** Low magnification. **b** High magnification of bottom of ZnO nanopillars. **c** High magnification of tip of ZnO nanopillars

Conclusions

In conclusion, we have synthesized nearly monodispersed ITO nanoparticles using a benign solvent (oleyl alcohol) and produced ink that is suitable for forming thin films by spin coating. The deposited ITO nanoparticles film showed high enough conductivity for transparent electrodes and can be coated onto high-aspect-ratio substrates. The ITO nanoparticle ink offers a number of advantages as a deposition method of transparent electrode onto a variety of structured substrates for technologically important applications.

Acknowledgments We thank Dr. Stephen L. Golledge for assistance in acquiring all XPS analysis reported in this work and Dr. Erik K. Richman for helpful discussions. We gratefully acknowledge Sony Corporation (Japan) for their support of this research. Portions of this work were also supported by the Air Force Research Laboratory (under agreement number FA8650-05-1-5041). The CAMCOR TEM facility is supported in grants from the W. M. Keck Foundation, the M. J. Murdock Charitable Trust, the Oregon Nanoscience and Microtechnologies Institute and the University of Oregon.

References

Argun AA, Cirpan A, Reynolds JR (2003) The first truly all-polymer electrochromic devices. Adv Mater 15(16):1338

Ba J, Fattakhova Rohlfing D, Feldhoff A, Brezesinski T, Djerdj I, Wark M, Niederberger M (2006) Nonaqueous synthesis of uniform indium tin oxide nanocrystals and their electrical

conductivity in dependence of the tin oxide concentration. Chem Mater 18(12):2848

Bechinger C, Ferrere S, Zaban A, Sprague J, Gregg BA (1996) Photoelectrochromic windows and displays. Nature 383:608

Bühler G, Thölmann D, Feldmann C (2007) One-pot synthesis of highly conductive indium tin oxide nanocrystals. Adv Mater 19(17):2224

Caruntu D, Yao K, Zhang Z, Austin T, Zhou W, O'Connor CJ (2010) One-step synthesis of nearly monodisperse, variable-shaped In_2O_3 nanocrystals in long chain alcohol solutions. J Phys Chem C 114(11):4875

Chen B, Sun XW, Tan S (2005) Transparent organic light-emitting devices with LiF/Mg:Ag cathode. Opt Express 13(3):937

Donley C, Dunphy D, Paine D, Carter C, Nebesny K, Lee P, Alloway D et al (2002) Characterization of indium–tin oxide interfaces using X-ray photoelectron spectroscopy and redox processes of a chemisorbed probe molecule: effect of surface pretreatment conditions. Langmuir 18(2):450

Fan JCC, Goodenough JB (1977) X-Ray photoemission spectroscopy studies of Sn-doped indium-oxide films. J Appl Phys 48(8):3524

Gilstrap RA Jr, Summers CJ (2009) Synthesis and analysis of an indium tin oxide nanoparticle dispersion. Thin Solid Films 518(4):1136

Gilstrap RA, Capozzi CJ, Carson CG, Gerhardt RA, Summers CJ (2008) Synthesis of a nonagglomerated indium tin oxide nanoparticle dispersion. Adv Mater 20:4163

Goebbert C, Nonninger R, Aegerter MA, Schmidt H (1999) Wet chemical deposition of ATO and ITO coatings using crystalline nanoparticles redispersable in solutions. Thin Solid Films 351(1–2):79

Hecht DS, Hu L, Irvin G (2011) Emerging transparent electrodes based on thin films of carbon nanotubes, graphene, and metallic nanostructures. Adv Mater 23(13):1482

Ho BPKH, Granström M (1998) Ultrathin self-assembled layers at the ITO interface to control charge injection and electroluminescence efficiency in polymer light-emitting diodes. Adv Mater 10:769–774

Ho P, Kim J, Burroughes J, Becker H, Li S, Brown T, Cacialli F et al (2000) Molecular-scale interface engineering for polymer light-emitting diodes. Nature 404(6777):481

Ito D, Jespersen ML, Hutchison JE (2008) Selective growth of vertical ZnO nanowire arrays using chemically anchored gold nanoparticles. ACS Nano 2(10):2001

Jeong J-A, Lee J, Kim H, Kim H-K, Na S-I (2010) Ink-jet printed transparent electrode using nano-size indium tin oxide particles for organic photovoltaics. Sol Energy Mater Sol Cells 94(10):1840

Kim Keun Soo, Zhao Y, Jang H, Lee SY, Kim JM, Kim KS, Ahn J-H et al (2009) Large-scale pattern growth of graphene films for stretchable transparent electrodes. Nature 457(7230):706

Krebs FC (2009) Polymer solar cell modules prepared using roll-to-roll methods: knife-over-edge coating, slot-die coating and screen printing. Sol Energy Mater Sol Cells 93(4):465

Li Y, Liu Z, Li Q, Liu Z, Zeng L (2011) Recovery of indium from used indium–tin oxide (ITO) targets. Hydrometallurgy 105(3–4):207

Lin Y-J, Hsu C-W, Chen Y-M, Wang Y-C (2005) Increase mechanism of indium-tin-oxide work function by KrF excimer laser irradiation. J Electron Mater 343:9

Minami T (2005) Transparent conducting oxide semiconductors for transparent electrodes. Semicond Sci Technol 20(4):S35

Otabe T, Ueda K, Kudoh A, Hosono H, Kawazoe H (1998) n-type electrical conduction in transparent thin films of delafossite-type AgInO[sub 2]. Appl Phys Lett 72(9):1036

Spaid M (2012) Wet-processable transparent conductive materials. Inf Disp 28(1):10

Sun Z, He J, Kumbhar A, Fang J (2010) Nonaqueous synthesis and photoluminescence of ITO nanoparticles. Langmuir 26(6):4246

Tahar RBH, Ban T, Ohya Y, Takahashi Y (1998) Tin doped indium oxide thin films: electrical properties. J Appl Phys 83:2631

Tvingstedt K, Inganäs O (2007) Electrode grids for ITO free organic photovoltaic devices. Adv Mater 19(19):2893

Zhu R, Kumar A, Yang Y (2011) Polarizing organic photovoltaics. Adv Mater 23(36):4193